J Solid State Electrochem (2010) 14:1595–1600
DOI 10.1007/s10008-009-0990-3

ORIGINAL PAPER

Direct electrochemistry and biocatalysis of glucose oxidase immobilized on magnetic mesoporous carbon

Jingjing Yu · Jiaxing Tu · Faqiong Zhao · Baizhao Zeng

Received: 10 August 2009 / Revised: 24 November 2009 / Accepted: 8 December 2009 / Published online: 5 January 2010

Abstract A magnetic mesoporous carbon material (i.e., mesoporous iron oxide/C, mesoFe/C) is synthesized for protein immobilization, using glucose oxidase (GOx) as model. Transmission electron microscopy images show that mesoFe/C has highly ordered porous structure with uniform pore size, and iron oxide nanoparticles are dispersed along the wall of carbon. After adsorption of GOx, the GOx-mesoFe/C composite is separated with magnet. The immobilized GOx remains its natural structure according to the reflection–absorption infrared spectra. When the GOx-mesoFe/C composite is coated on a Pt electrode surface, the GOx gives a couple of quasireversible voltammetric peaks at −0.5 V (vs. saturated calomel electrode) due to the redox of FAD/$FADH_2$. The electron-transfer rate constant (k_s) is ca. 0.49 s^{-1}. The modified electrode presents remarkably amperometric response to glucose at 0.6 V. The response time ($t_{95\%}$) is less than 6 s; the response current is linear to glucose concentration in the range of 0.2–10 mM with a sensitivity of 27 μA $mM^{-1} cm^{-2}$. The detection limit is 0.08 mM (S/N=3). The apparent Michaelis–Menten constant (K_m^{app}) of the enzyme reaction is ca. 6.6 mM, indicating that the GOx immobilized with mesoFe/C has high affinity to the substrate.

Keywords Magnetic mesoporous carbon · Glucose oxidase · Direct electrochemistry · Biocatalysis · Glucose

Electronic supplementary material The online version of this article (doi:10.1007/s10008-009-0990-3) contains supplementary material, which is available to authorized users.

J. Yu · J. Tu · F. Zhao (✉) · B. Zeng
Department of Chemistry, Wuhan University,
Hubei Province,
Wuhan 430072, People's Republic of China
e-mail: fqzhao@whu.edu.cn

Introduction

The direct electrochemistry of redox proteins has received considerable attention in last two decades [1–5]. However, the direct electron transfer between redox proteins and electrode surface is generally difficult because the active centers of proteins are usually deeply embedded in protein molecules and the strong adsorption of proteins on electrode surface easily leads to their denaturation. To realize the direct electron transfer between proteins and electrode, various materials were adopted to immobilize redox proteins on electrode surface, such as surfactants [6], polymers [7], sol-gel [8], nanoparticles [9–11], mesoporous materials [12, 13], and so on.

Among these materials, magnetic and mesoporous materials have attracted increasing interest of researchers. The main advantage of magnetic material as immobilizing material is the simple procedure to separate the immobilized biomolecules from the reactant mixture [14]. The direct electrochemistry of heme-proteins was achieved by immobilizing them with Fe_3O_4-based magnetic materials [15, 16]. As for mesoporous materials, they are thought to be very suitable for biomacromolecule immobilization because they possess high surface area and large pore volume as well as mechanical and chemical resistance [17]. In addition, the molecular crowding theory and modeling efforts have predicted that a protein inside a confined space would be more stable due to some folding forces in comparison with that in bulk solutions [18]. Hence, mesoporous materials have high loading amount and may enhance the stability of proteins. Several mesoporous materials, such as mesoporous silica–carbon nanocomposite [13], mesoporous carbon [19], mesoporous TiO_2 [20], mesoporous Al_2O_3 [21], were employed to immobilize redox proteins on electrode surface. The immobilized

proteins showed direct electrochemical behavior, high stability, and bioactivity [13, 19–21].

Taking into account the advantages of the two types of material, a magnetic mesoporous carbon material (i.e., mesoporous iron oxide/C) is synthesized for protein immobilization in this work, with glucose GOx as model. Previously, Lee et al. [22] employed magnetic mesocellular carbon foam as enzyme immobilization matrix to fabricate redox mediator-based glucose biosensor, which showed magnetically switchable electrocatalysis to glucose. However, as far as we know, the direct electrochemistry of GOx immobilized on magnetic mesoporous carbon has not been reported.

Experimental

Reagents

GOx (21.7 $U mg^{-1}$, Mr 186000) was purchased from Fluka. Furfuryl alcohol and glucose were from Sinopharm Chemical Reagent Co., Ltd. (Shanghai, China). Nafion solution was prepared by diluting 5% Nafion DE 520 (DuPont, USA) solution with ethanol. Other chemicals used were of analytical grade, and the solutions were prepared with deioned water.

Synthesis of mesoFe/C

MesoFe/C composite was synthesized according to the literature [23], using mesoporous silica SBA-15 as hard template, $FeCl_3 \cdot 6H_2O$ as iron source, and furfuryl alcohol as carbon source. Typically, 1.5 ml of furfuryl alcohol and 7.5 mg oxalic acid were dissolved in 10 ml ethanol. Following, 1 g SBA-15 was added into the solution, and it was stirred for 0.5 h. The resulting mixture was treated at 363 K for 12 h and then at 423 K for 6 h. To introduce iron oxide into the composite, 0.86 g $FeCl_3 \cdot 6H_2O$ dissolved in 10 ml ethanol was mixed with the composite obtained above and then stirred for 0.5 h. After evaporating the ethanol, the resulting composite was thermal-treated in N_2 at 873 K for 4 h to carbonize the furfuryl alcohol. The silica template in the composite was removed through twice washing with heated 2 M NaOH solution. The mixture was filtered, washed with water and ethanol, and dried at 333 K. Thus, mesoFe/C was obtained.

Preparation of GOx-mesoFe/C composite and modified electrode

Five micrograms of mesoFe/C composite was mixed with 0.5 ml 30 mg ml^{-1} GOx aqueous solution and the mixture was kept at 4 °C for 48 h to establish adsorption equilibrium. The GOx-mesoFe/C composite was separated from the mixture by magnetic decantation and washed with water for three times, and then dried at 313 K under vacuum for 12 h. For electrode modification, the GOx-mesoFe/C composite was dispersed in 1 ml water again. Before modification, a platinum electrode was polished to mirror smooth with 0.05 μm Al_2O_3 slurry, rinsed with water, and then ultrasonicated in water bath. Three microliters of GOx-mesoFe/C suspension was transferred onto the platinum electrode surface and was dried in air. One microliter of 0.5% Nafion was added on the modified electrode surface to enhance its mechanical stability. The obtained electrode was denoted as GOx-mesoFe/C-Nafion/Pt. For comparison, mesoFe/C-Nafion/Pt was prepared through similar way.

Apparatus

All electrochemical experiments were performed on a CHI 660A electrochemical workstation (CH Instru. Co., Shanghai, China) under room temperature (25±2 °C). The electrode system was composed of a modified Pt electrode (2 mm in diameter), a platinum auxiliary electrode, and a saturated calomel electrode (SCE). The amperometric response to glucose was measured at an applied potential of 0.6 V (vs. SCE) in air-saturation phosphate buffer solution (PBS, pH 6.98) under stirred condition. After the background current reached steady-state value, glucose was injected stepwise into the solution and the current was recorded.

Transmission electron microscopy (TEM) images were obtained on a JEM-2010FEF electron microscope (Japan). Energy-dispersive X-ray spectra (EDX) were collected from the attached energy-dispersive spectrometer. The adsorption and desorption experiments of N_2 were performed on a SA 3100 surface area and pore size analyzer (Beckman Coulter, USA). The specific surface area and pore volume were estimated by applying Brunauer–Emmett–Teller (BET) method [24]. Reflection–absorption infrared (RAIR) spectra were obtained using a Nicolet FTIR-360 spectrometer (USA).

Results and discussion

Characterization of mesoFe/C and GOx-mesoFe/C

Figure 1a displays the TEM images of mesoFe/C, which shows highly ordered porous structure with pore diameter of about 3–4 nm. The darker parts in the mesoFe/C composite framework are believed to be iron oxide nanoparticles, and they are dispersed along the wall of carbon (Fig. 1a inset). EDX spectrum of mesoFe/C indicates that there are Fe, O, C, and Cu in the composite (Fig. 1b). The source of Cu is the copper grid and C is the mesoporous carbon. The iron oxide

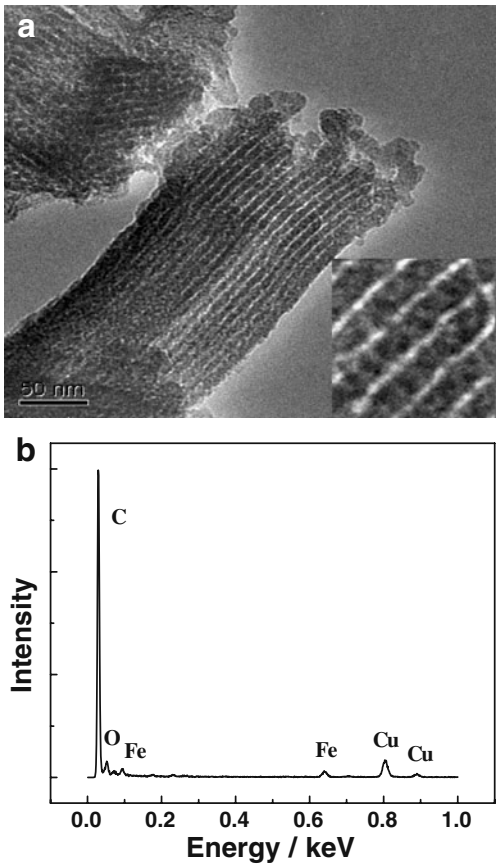

Fig. 1 TEM images (**a**) and EDX (**b**) of mesoFe/C. *Inset* shows the magnified image of **a**

results from the decomposition of $FeCl_3 \cdot 6H_2O$ at 873 K in N_2 [21]. The magnetism of mesoFe/C composite can be attributed to the iron oxide nanoparticles. Mesoporous carbon actually acts as shield of iron oxide nanoparticles [25]. On the other hand, the iron oxide nanoparticles loaded in carbon wall will not block pores or influence mass transfer. In addition, the specific surface area of mesoporous carbon does not decrease after loading iron oxide nanoparticles. The protein adsorption on mesoFe/C is tested using GOx as model (Fig. 2). As can be seen, the yellow GOx solution becomes light (Fig. 2c), indicating that GOx is adsorbed on mesoFe/C. The resulting GOx-mesoFe/C composite is magnetic and can be attracted by a magnet, which is favorable for their separation. The enzyme amount adsorbed is ca. 470 mg g^{-1} according to the increase in mesoFe/C weight after adsorbing GOx.

To obtain the information about pore structure and specific surface area of mesoFe/C and GOx-mesoFe/C, N_2 adsorption/desorption experiments are performed (Fig. 3a). At relative pressure (p/p_0) in the range of 0.4–0.8, the isotherm of mesoFe/C gives a sharp rise and produces a hysteresis loop. This is a type IV curve of mesoporous materials. The BET surface area and pore volume are calculated to be 709 $m^2 g^{-1}$

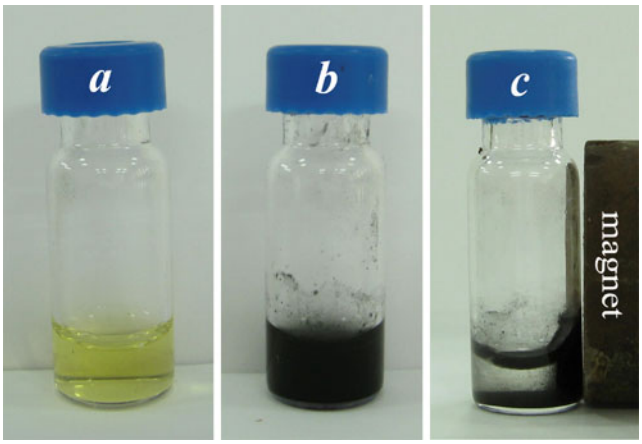

Fig. 2 Photos of GOx solution (**a**), GOx and mesoFe/C mixture (**b**), and GOx-mesoFe/C composite attracted by a magnet after 48 h adsorption (**c**)

and 1.04 $cm^3 g^{-1}$, respectively. After the adsorption of GOx, the isotherm of GOx-mesoFe/C is still type IV curve, but shows smaller rise compared with that of mesoFe/C. It indicates that mesoFe/C remains porous structure after

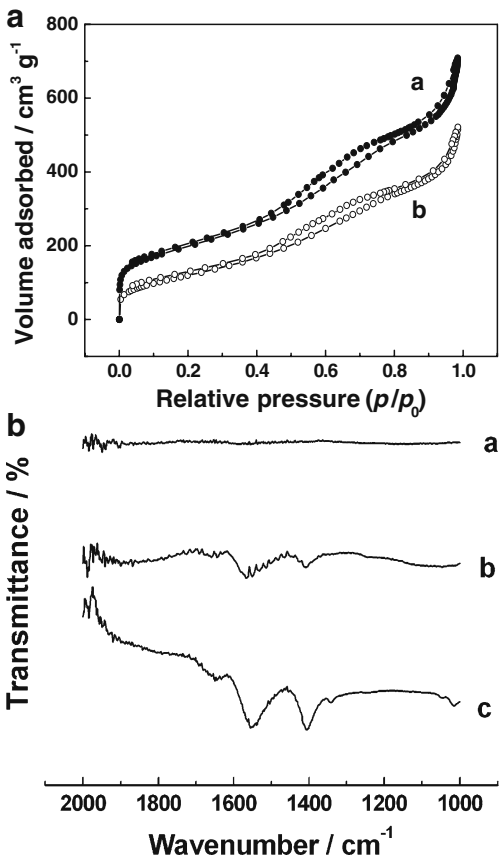

Fig. 3 **a** N_2 adsorption–desorption isotherm curves of mesoFe/C (*a*) and GOx-mesoFe/C composite (*b*); **b** RAIR spectra of mesoFe/C (*a*), GOx-mesoFe/C (*b*), and GOx (*c*) on glassy carbon surface

adsorbing GOx, and the BET surface area and pore volume decrease obviously. They are 439 $m^2 g^{-1}$ and 0.76 $cm^3 g^{-1}$, respectively. RAIR spectra are used to explore the secondary structure of GOx immobilized on mesoFe/C [13, 26]. As shown in Fig. 3b, the absorption bands in the range of 1,800–1,000 cm^{-1} are assigned to the characteristic peaks of stretching vibration of carbonyl groups, bending vibration of amide groups, methyl and methylene groups, and sugar rings in GOx (curve c) [26]. The mesoFe/C does not show significant absorption bands in the range (curve a). However, the absorption bands of GOx-mesoFe/C composite are similar to that of GOx (curve b). This indicates that the immobilized GOx remains its native structure.

Direct electrochemistry of immobilized GOx

Figure 4 shows the cyclic voltammograms (CVs) of GOx-mesoFe/C-Nafion composite and mesoFe/C-Nafion modified electrodes. The mesoFe/C-Nafion modified electrode does not exhibit any peaks under the given conditions. However, the GOx-mesoFe/C-Nafion composite modified electrode shows a pair of redox peak, which is undoubtedly caused by the FAD/$FADH_2$ couple of GOx. The cathodic (E_{pc}) and anodic (E_{pa}) peak potentials are −0.516 and −0.483 V, respectively. Thus, the formal potential (defined as the average of anodic and cathodic peak potentials) is −0.50 V. The peak-to-peak separation (ΔE_p) is 33 mV, and the anodic (i_{pa}) and cathodic peak (i_{pc}) currents are almost equal, implying that the immobilized GOx undergoes a quasireversible electrochemical reaction [6].

With scan rate increasing from 5 to 90 mV s^{-1}, the peak currents increase linearly, but the peak potentials keep almost unchanged (Fig. 5). The regression equations are $i_{pc} = 0.02 + 15.3\upsilon(\mu A, V\,s^{-1}, r = 0.996)$ and $i_{pa} = -0.01 - 15.5\upsilon(\mu A, V\,s^{-1}, r = 0.990)$. Furthermore, the log i_{pc}–log υ and log i_{pa}–log υ plots are linear and the ratio of the slopes is about one. These indicate that the electrochemical reaction of GOx immobilized on mesoFe/C is surface-controlled [7]. However, the charge consumed in coulomb (Q), obtained from integrating cathodic peak area of CVs, keeps almost unchanged. This reflects the electrochemical characteristic of a thin layer system. Thus, the surface concentration (Γ^*) of electroactive protein can be calculated and it is 3.7×10^{-11} mol cm^{-2} according to the equation $Q = nFA\Gamma^*$ [7], where A is the electroactive area of electrode obtained from Randles–Sevcik equation [27]. In comparison with the total surface concentration of GOx immobilized on electrode surface (estimated to be 1.18×10^{-9} mol cm^{-2}), there is about 3.14% of the immobilized GOx taking part in the electrochemical reaction. As the theoretical monolayer coverage for GOx is about 4.7×10^{-12} mol cm^{-2} [28], it can be proposed that several layers of the immobilized GOx undergo electrochemical reaction.

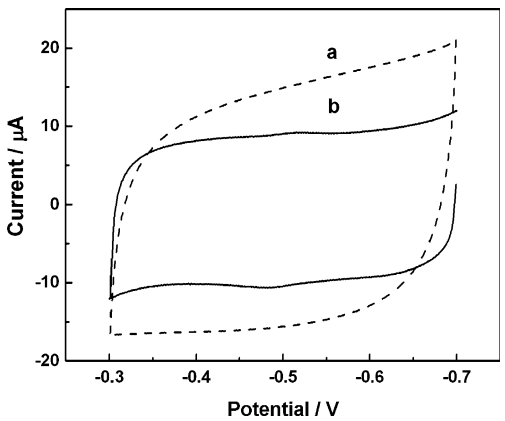

Fig. 4 CVs of mesoFe/C-Nafion/Pt (**a**) and GOx-mesoFe/C-Nafion/Pt (**b**) electrodes in 0.10 M deoxygenated PBS (pH6.98). *Scan rate* is 20 mV s^{-1}

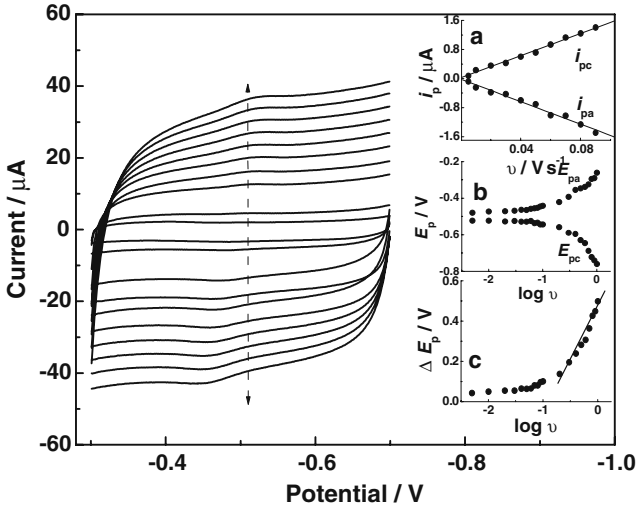

Fig. 5 CVs of GOx-mesoFe/C-Nafion/Pt at different scan rate (υ, from inner to outer: 5, 10, 20, 30, 40, 50, 60, 70, 80, and 90 mV s^{-1}). *Insets* show the plots of i_p vs. υ (*a*), E_p vs. log υ (*b*), and ΔE_p vs. log υ (*c*). Other conditions are the same as those in Fig. 4

When scan rate exceeds 90 mV s^{-1}, the peak separation increases gradually (Fig. 5b). Furthermore, ΔE_p and logarithm of scan rate show linear relationship as shown in Fig. 5c. According to the following equation [29],

$$\Delta E_p = \frac{2.3RT}{(1-\alpha)\alpha nF} \times \left\{ \begin{matrix} \alpha\log(1-\alpha) + (1-\alpha) \\ \log\alpha - (1-2\alpha)\log\dfrac{RT}{nF} - (1-2\alpha)\log k_s \end{matrix} \right\} + \frac{2.3RT(1-2\alpha)}{(1-\alpha)\alpha nF}\log\upsilon$$

Where α is the electron-transfer coefficient and other symbols have their normal significance. As n is 2 [10], the

electron-transfer rate constant (k_s) of GOx is ca. 0.49 s^{-1}. The value is smaller than the corresponding value observed for GOx immobilized on conductive mesocellular silica–carbon nanocomposite foam (i.e., 14.0±1.7 s^{-1}) [13], but nears that on single-walled carbon nanotube modified electrode (i.e., 0.3 s^{-1}) [9]. It was reported that the direct electrochemistry of GOx with k_s larger than 0.1 s^{-1} could be observed when the distance between the electrode and the FAD was less than that (i.e., 13 Å) between FAD and the surface of the enzyme in its native configuration [30]. Thus, the interaction between GOx and mesoFe/C makes the distance between redox center and electrode decrease, promoting the direct electron transfer of GOx.

The CVs change significantly with solution pH (data not shown). When solution pH increases from 4.92 to 9.18, the redox peaks shift negatively. The formal potential is linear to pH value with a slope of −0.046 V pH^{-1}, which is close to the theoretical value of −0.059 V pH^{-1} for the electrochemical reaction with equal numbers of transferred proton and electron [27]. Therefore, the electrochemical reaction of GOx involves two-electron and two-proton transfer.

Biocatalysis of the immobilized GOx

To demonstrate the biocatalytic activity of the immobilized GOx, the response of GOx-mesoFe/C-Nafion modified electrode to glucose is examined. As shown in Fig. 6a, under aerobic condition, the enzyme electrode shows larger cathodic current compared with its anodic current, indicating the electrocatalytic reduction of dissolved oxygen. With glucose concentration increasing, the cathodic current decreases gradually due to the consumption of dissolved oxygen as expressed in the following equations [31]:

$$\mathrm{GOx(FAD)+glucose \rightleftarrows gluconolactone + GOx(FADH_2)} \quad (1)$$

$$\mathrm{GOx(FADH_2)+O_2 \rightleftarrows GOx(FAD)+H_2O_2} \quad (2)$$

However, the change is not as distinct as that reported previously [13] and cannot be used for quantitive determination. The probable reason is that only a small part of GOx (i.e., 3.14%) takes part in the direct electrochemistry.

The amperometric response to glucose at an applied potential of 0.6 V is recorded (Fig. 6b). The mesoFe/C-Nafion modified electrode does not respond to the addition of glucose. However, GOx-mesoFe/C-Nafion modified electrode gives remarkably response to glucose, resulting from the electrochemical oxidation of H_2O_2 produced by enzyme-catalyzed reaction as mentioned above. Obviously, the GOx which does not take part in the direct electrochemistry shows bioactivity also. The current response is

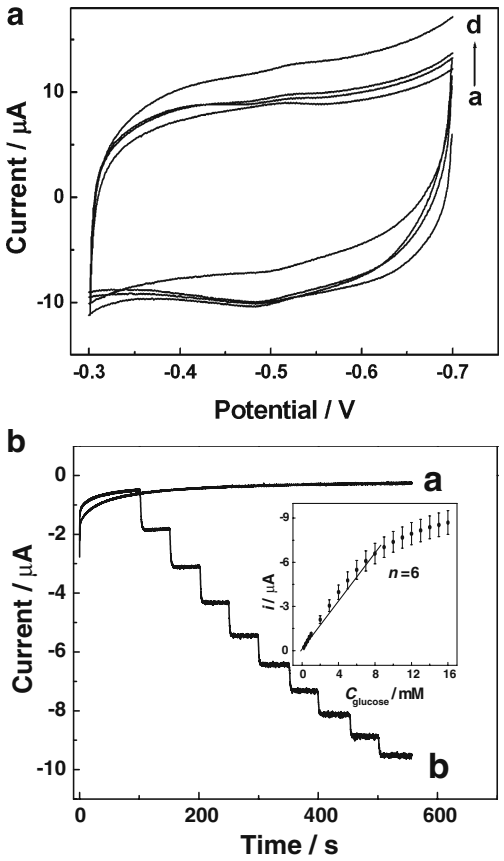

Fig. 6 **a** CVs of GOx-mesoFe/C-Nafion/Pt in 0.10 M deoxygenated PBS (*a*) and air-saturated PBS (*d*) plus 2 mM (*c*) and 4 mM (*b*) glucose. *Scan rate* is 20 mV s^{-1}. **b** Amperometric response of mesoFe/C-Nafion/Pt (*a*) and GOx-mesoFe/C-Nafion/Pt (*b*) to the injection of 1 mM glucose in air-saturated PBS at an applied potential of 0.6 V. *Inset* shows the calibration curve

fast and the response time ($t_{95\%}$) is less than 6 s. The response current is linear to glucose concentration in the range of 0.2–10 mM, and the regression equation is $i = 0.079 + 0.865\, c_{\mathrm{glucose}}(\mu\mathrm{A}, \mathrm{mM}, r = 0.990, n = 6)$. The sensitivity is 27 μA $mM^{-1}cm^{-2}$, the detection limit is 0.08 mM (*S/N*=3). At higher glucose concentration, the response shows the characteristics of Michaelis–Menten kinetic mechanism [32]. The apparent Michaelis–Menten constant (K_m^{app}) of the enzyme reaction at GOx-mesoFe/C-Nafion modified electrode is ca. 6.6 mM. This value is smaller than 10.8 mM for GOx immobilized with Pt nanoparticles–mesoporous carbon [33] and 27 mM for native GOx in solution [34]. It reveals that the immobilized GOx has high affinity to the substrate.

Reproducibility and stability of GOx-mesoFe/C modified electrode

The reproducibility of GOx-mesoFe/C-Nafion/Pt is evaluated by comparing the response currents of five enzyme

electrodes prepared under the same conditions. The relative standard deviation (RSD) of response current for 1 mM glucose is 5.7%. One enzyme electrode is used in 20 successive measurements and the RSD is 1.4%. When the enzyme electrode is stored in PBS (pH6.98) at 4°C, it retains 90.3% of its initial response current after 1 week. These indicate that the GOx-mesoFe/C-Nafion/Pt has good reproducibility and stability.

Conclusions

The synthesized mesoFe/C has high specific surface area, large pore volume, and strong magnetic, which is suitable for protein immobilization and separation. GOx can be immobilized on the mesoFe/C and it keeps natural structure. The direct electrochemistry of the immobilized GOx is achieved when it is coated on a Pt electrode. What is more, the immobilized GOx shows high biocatalysis to glucose and can be used to construct glucose biosensor.

Acknowledgments The authors appreciate the support from the National Natural Science Foundation of China (grant number: 20173040) and the State Key Laboratory of Chem/Biosensing and Chemometrics, Hunan University, Changsha, People's Republic of China.

References

1. Gooding JJ, Wibowo R, Liu JQ, Yang WR, Losic D, Orbons S, Mearns FJ, Shapter JP, Hibbert DB (2003) J Am Chem Soc 125:9006
2. Boussaad S, Tao NJ (1999) J Am Chem Soc 121:4510
3. Zhou YL, Hu NF, Zeng YH, Rusling JF (2002) Langmuir 18:211
4. Armstrong FA, Heering HA, Hirst J (1997) Chem Soc Rev 26:169
5. Li JW, Liu LQ, Xiao F, Gui Z, Yan R, Zhao FQ, Hu L, Zeng BZ (2008) J Electroanal Chem 613:51
6. Mimica D, Zagal JH, Bedioui F (2001) J Electroanal Chem 497:106
7. Lu Q, Zhou T, Hu SS (2007) Biosens Bioelectron 22:899
8. Nadzhafova O, Etienne M, Walcarius A (2007) Electrochem Commun 9:1189
9. Liu J, Chou A, Rahmat W, Paddon-Row MN, Gooding JJ (2005) Electroanal 17:38
10. Cai CX, Chen J (2004) Anal Biochem 332:75
11. Wu H, Wang J, Kang XH, Wang CM, Wang DH, Liu J, Aksay IA, Lin YH (2009) Talanta 80:403
12. You CP, Xu X, Tian BZ, Kong JL, Zhao DY, Liu BH (2009) Talanta 78:705
13. Wu S, Ju H, Liu Y (2007) Adv Funct Mater 17:585
14. Li J, Gao H (2008) Electroanal 20:881
15. Cao D, Hu N (2006) Biophys Chem 121:209
16. Zhao G, Xu JJ, Chen HY (2006) Electrochem Commun 8:148
17. Wang Y, Caruso F (2005) Chem Mater 17:953
18. Lei C, Shin Y, Magnuson JK, Fryxell G, Lasure LL, Elliott DC, Liu J, Ackerman EJ (2006) Nanotechnology 17:5531
19. Feng JJ, Xu JJ, Chen HY (2007) Biosens Bioelectron 22:1618
20. Jia NQ, Wen YL, Yang GF, Lian Q, Xu CJ, Shen HB (2008) Electrochem Commun 10:774
21. Yu JJ, Ma JR, Zhao FQ, Zeng BZ (2007) Electrochim Acta 53:1995
22. Lee J, Lee D, Oh E, Kim J, Kim Y, Jin S, Kim H, Hwang Y, Kwak JH, Park J, Shin C, Kim J, Hyeon T (2005) Angew Chem Int Ed 44:7427
23. Dong X, Chen H, Zhao W, Li X, Shi J (2007) Chem Mater 19:3484
24. Barrett EP, Joyner PH, Halenda PP (1951) J Am Chem Soc 73:373
25. Pan J, Yang Q (2007) Anal Bioanal Chem 388:279
26. Shan D, Zhu M, Xue H, Cosnier S (2007) Biosens Bioelectron 22:1612
27. Hodak J, Etchenique R, Calvo EJ (1997) Langmuir 13:2708
28. Laviron E (1979) J Electroanal Chem 101:19
29. Hecht HJ, Schomburg D, Kalisz H, Schmid RD (1993) Biosens Bioelectron 8:197
30. Bard AJ, Faulkner LR (2001) Electrochemical methods: fundamentals and applications. John Wiley & Sons, New York
31. Yao YL, Shiu KK (2008) Electroanal 20:1542
32. Kamin RA, Wilson GS (1980) Anal Chem 52:1198
33. Yu JJ, Yu DL, Zhao T, Zeng BZ (2008) Talanta 74:1586
34. Rogers MJ, Brandt KG (1971) Biochemistry 10:4624